Functionally Graded Lattice Walls via Continuous Eulerian Toolpaths for Robotic 3D Concrete Printing

Christopher J. Watson[1] [0009−0007−0764−9469], Kira Barton[1] [0000−0003−1047−8078], and Mania Aghaei Meibodi[2] [0000−0003−2867−6814]

[1] University of Michigan, Robotics Department, Barton Research Group, Ann Arbor, MI, USA
cjwatson@umich.edu, bartonkl@umich.edu
[2] University of Michigan, Taubman College of Architecture and Urban Planning, DART Lab, Ann Arbor, MI, USA
meibodi@umich.edu

Abstract. This paper introduces a computational framework for generating and printing functionally graded lattice walls using a single uninterrupted toolpath in extrusion-based 3D concrete printing. The approach addresses a key limitation in current 3DCP practice: graded or heterogeneous reticulated designs typically require multiple segmented toolpaths, introducing pauses that degrade interlayer adhesion and destabilize deposition. Our framework eliminates these interruptions by ensuring that every edge of the graded lattice is visited exactly once in a geometrically directed Eulerian trail. The method combines a banded macrocell representation—used to assign locally varying lattice densities—with a diamond-cell decomposition that guarantees printable spacing across density transitions. To traverse these non-uniform lattice graphs without retractions, we develop a modified Eulerian strategy that inserts a single stitch node, assigns consistent start–stop nodes, and links consecutive layers through nearest-node continuation. Together, these elements produce a fully continuous multi-layer trajectory governed entirely by geometric rules. We validate the method by fabricating a 1.00 m × 0.60 m × 0.35 m functionally graded lattice wall comprising 35 layers. The printed artifact demonstrates clear density transitions, consistent vertical alignment, and continuous deposition maintained throughout the build. The results confirm that computational geometry and geometrically directed graph traversal enable reliable, continuous printing of complex graded lattices at architectural scale.

1 Introduction

Robotic 3D concrete printing (3DCP) is a technology that offers new methods for shaping and producing formwork-free construction for concrete structures that are materially efficient at an architectural scale [1]. Given this context, lattice and grid-filled wall systems have gained attention for weight reduction and tunable mechanical performance [2]. These applications are limited significantly by deposition continuity and toolpath generation.

Existing lattice infill strategies rely on segmented or layer-wise toolpaths that require frequent start-stop operations, retractions, and region-based decomposition to accommodate density or topology changes [3]. In extrusion-based printing, these interruptions disrupt material flow and weaken interlayer bonding, with pronounced effects in heterogeneous designs where spatial variation can require multiple disconnects per layer.

Although recent research has explored near-continuous path strategies for concrete printing to include medial-axis decomposition, transfinite mapping, and global path optimization for branched geometries [3], they do not address graph-theoretic constraints imposed by non-uniform lattice networks. Thus functionally graded lattice networks, which have great structural and material efficiency, use discretized paths which can compromise print quality.

This paper addresses this gap by introducing a computational framework for generating functionally graded lattice walls that are printable with a single uninterrupted toolpath. By treating the lattice not as a geometry to be filled, but rather a traversable graph, a Eulerian traversal can be enforced. Ensuring Eulerian traversability eliminates retractions by construction, rather than by heuristic post-processing. This approach combines geometric lattice design with graph-theoretic path planning to enable reliable fabrication of complex graded structures without pauses or segmentation strategies.

Contributions

1. Geometric framework for banded lattice generation.
2. Modified Eulerian traversal producing continuous paths.
3. Full-scale fabrication of a functionally graded lattice wall.

The primary contribution of this work is not geometric novelty but the enforcement of continuous material deposition as a first-class fabrication constraint.

2 Background

2.1 Reticulated Patterns and Functional Porosity

Although reticulated patterns have been used for a long time in structural systems to reduce material usage while maintaining performance-driven parameters, 3DCP enables formwork-free printing of lattice and grid-filled patterns. These patterns can be used to introduce porosity, reduce weight, and tailor local stiffness and structural load transfer [2,4]. Recent work has shown that ribbed and reticulated concrete systems derived from stress fields enable encoding of structural intent directly into the printed form [5].

Despite these advances most lattice systems rely on uniform cell distribution or discrete pattern changes in localized scales. Fine-grained functional grading remains a challenge in practice, not as a fault of geometric modeling alone, but due to fabrication implications that complicate the process.

2.2 Concrete Extrusion Constraints

Extrusion-based concrete is highly sensitive to process continuity. Unlike plastic-based extrusion, concrete deposition has a time-sensitive rheology, limited open-time, and is sensitive to changes in acceleration [6]. Disruptions in deposition can weaken interlayer bonding and promote overbuild at junctions.

Some studies have shown that interlayer bonding in printed concrete is strongly tied to time gaps between each layer and adjacent filament [7]. Even a short pause can reduce bond strength and introduce likely failure points. Further review of large-scale additive manufacturing in concrete emphasizes that geometric complexity must complement stable, continuous deposition—particularly in architectural-scale builds where cumulative process effects become critical [8,1].

2.3 Toolpath-centric design

To handle these fabrication constraints some research has argued for a shift from geometry-first modeling to toolpath-centric design. Breseghello and Naboni [9] propose that the toolpath itself should be a primary design driver for concrete structures, rather than a downstream artifact. Complementary work has shown that computational geometry and fabrication-aware workflows can encode structural intent directly into printable toolpath trajectories [5]. Yet most approaches still rely on segmented toolpaths when used with heterogeneous or graded geometries, which becomes a limitation for a continuous lattice system.

2.4 Eulerian Pathing in Additive Manufacturing

Graph-based formulations provide a natural abstraction for lattice toolpaths: struts correspond to edges and intersections to nodes. In additive manufacturing, continuous traversal of sparse infill graphs has been shown to reduce retractions and improve deposition stability [10]. Related work on multi-axis, support-free deposition of lattice-filled geometries further highlights the coupling between lattice topology and toolpath planning [11]. Existing continuous infill methods assume uniform graphs; graded lattices violate Eulerian conditions due to odd-degree boundary nodes and local connectivity changes.

2.5 Positioning of this work

Three gaps remain. Existing methods do not guarantee a single uninterrupted toolpath for functionally graded lattice walls across density transitions and stacked layers, and no general geometric framework exists for fine-grained grading that preserves printable spacing while producing layer graphs suitable for continuous traversal. As a result, current fabrication-aware workflows rarely unify geometric grading and graph-theoretic traversal into one pipeline that enforces continuity as a first-class constraint.

3 Methods

To address the identified gaps, we introduce a unified geometry–topology–toolpath framework that integrates graded lattice generation with continuous path planning:

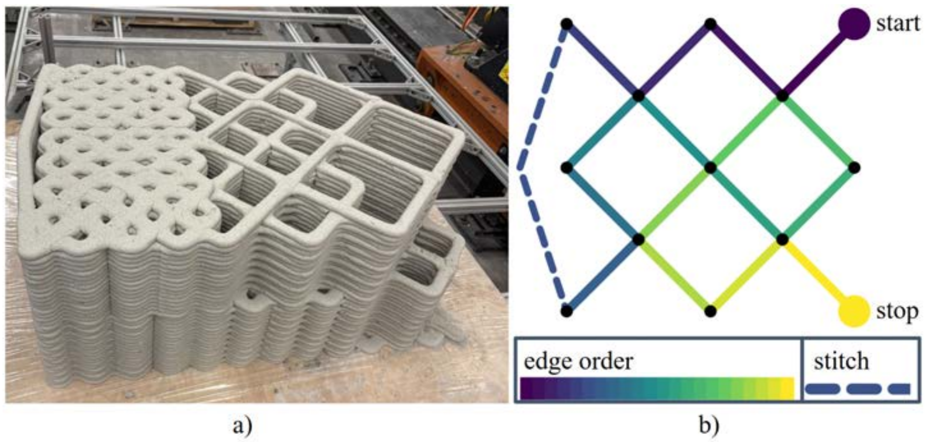

Fig. 1: Continuous single-layer toolpath planned as an Eulerian path. (a) Fabricated functionally graded lattice wall (1.00 × 0.60 × 0.35 m). (b) The layer is treated as a graph; since an Eulerian path requires exactly two odd-degree vertices, a stitch edge (dashed) joins the nearest degree-1 corners, reducing four odd nodes to two, which become the fixed start and stop. Edge color shows traversal order. Simplified for clarity.

1. **Banded lattice construction** using a hierarchical macrocell–subcell discretization to encode functional grading while enforcing printable spacing.
2. **Diamond-cell decomposition** producing planar layer graphs with deterministic node degrees and controlled boundary conditions.
3. **Stitched Eulerian traversal** that guarantees a single uninterrupted multi-layer toolpath without retractions.

3.1 Banded geometric lattice construction

Each layer is generated as a functionally graded lattice using a macrocell–subcell discretization. Let

$$\mathcal{G} = \big(M, \{s_b\}_{b\in\mathcal{B}}\big), \qquad s_b \mid M,$$

where M is the macrocell size and each band b specifies a subcell size s_b. A band field $B^{(k)}$ assigns a band index to each macrocell in layer k, encoding local lattice density.

Print-feasible spacing is enforced globally via a scale factor α derived from a target centerline distance d_{target}. For the diamond lattice,

$$\alpha = \frac{d_{\text{target}}}{D_{\text{unit}}}, \qquad D_{\text{unit}} = \frac{s_{\min}}{\sqrt{2}},$$

where $s_{\min} = \min_b s_b$. This guarantees that the densest lattice region satisfies spacing constraints and all coarser regions remain printable.

All layers share $(\mathcal{G}, \alpha)$ and spatial extents, ensuring deterministic reconstruction and vertical registration.

3.2 Diamond-cell decomposition and layer graph generation

Each subcell is expanded into a fixed diamond "X" topology consisting of one center node connected to four corner nodes. Adjacent subcells share corner nodes, which are merged deterministically using integer-coordinate hashing. After metric embedding, each layer forms a planar geometric graph

$$\mathcal{L}^{(k)} = (V^{(k)}, E^{(k)}).$$

This decomposition yields predictable node degrees: all interior nodes have even degree, while exactly four boundary nodes have degree 1 at the corners of the layer domain. As a result, each layer graph is planar, connected, and topologically constrained in a manner suitable for controlled Eulerian traversal, independent of local lattice density.

3.3 Stitched Eulerian traversal and continuous toolpath generation

The objective is a single uninterrupted toolpath that traverses every printable edge exactly once per layer and links layers without retractions. For layer k, define

$$\mathcal{S}^{(k)} = \{v \in V^{(k)} : \deg(v) = 1\}, \qquad |\mathcal{S}^{(k)}| = 4.$$

A geometrically directed Eulerian trail requires exactly two odd-degree nodes. We therefore eliminate two boundary odd nodes using a single stitch edge. The closest pair

$$(s_A, s_B) = \arg \min_{u<v \in \mathcal{S}^{(k)}} \|p(u) - p(v)\|_2$$

is selected and connected by one added edge, converting both nodes to even degree and leaving the remaining two boundary nodes as the start and stop of the layer traversal. The stitch is treated as a single graph edge and may be routed along the boundary during execution.

With exactly two odd-degree nodes, each layer admits a geometrically directed Eulerian trail, which is computed using a modified Hierholzer walk. When multiple unused edges are available, the traversal prioritizes non-bridge edges, limits repeated node visits, and favors short geometric steps. This produces an ordered vertex sequence

$$P^{(k)} = [v_0, v_1, \ldots, v_{T_k}],$$

that traverses every lattice edge exactly once. This is shown in Fig. 1.

To form a continuous multi-layer toolpath, the start node of layer $k+1$ is chosen as the node nearest to the endpoint of layer k:

$$v_{\text{start}}^{(k+1)} = \arg \min_{v \in V^{(k+1)}} \|p(v) - p_{\text{stop}}^{(k)}\|_2.$$

Concatenating all layer paths yields a single uninterrupted trajectory

$$P_{\text{global}} = P^{(0)} \| P^{(1)} \| \cdots \| P^{(N-1)},$$

enabling continuous deposition across the full wall height.

Table 1: Key geometric and process parameters used in the fabrication of the functionally graded lattice wall.

Parameter	**Value**
Wall dimensions (L × W × H)	1.00 m × 0.60 m × 0.35 m
Macrocell size M	64 units
Global scale factor α	0.00443 m/unit
Spacing target d_{target}	0.05 m
Subcell sizes (bands)	{64, 32, 16} units
Layer thickness	10 mm
Volumetric flow rate Q	2.8 L/min

3.4 Assumptions

The framework assumes that layer geometry is vertically registered so nearest-node linking produces feasible inter-layer transitions. This condition is satisfied by the banded diamond-cell construction used in this work.

4 Case Study

A functionally graded lattice wall was fabricated to validate the proposed geometry–topology–toolpath framework under continuous extrusion. The wall measures $1.00\ \text{m} \times 0.60\ \text{m} \times 0.35\ \text{m}$ and consists of 35 stacked planar lattice layers printed as a single uninterrupted toolpath. Lattice density varies spatially according to a prescribed grading function while all geometric and process parameters remain fixed across layers. Key geometric and fabrication parameters are summarized in Table 1.

4.1 Material and fabrication system

All experiments used Sikacrete®-752 3D, a commercially available thixotropic micro-concrete formulated for robotic extrusion. The material exhibits sufficient pumpability, shape retention, and early-age strength to support continuous lattice deposition at architectural scale.

Fabrication was performed using a 6-DOF industrial robotic arm equipped with a MAIMultiMix-3D extrusion system. Material was delivered through a progressive-cavity pump at a fixed volumetric flow rate of 2.8 L/min and extruded through a 25.4 mm circular nozzle. While the volumetric flow rate remained constant throughout fabrication, nozzle motion was locally modulated through velocity control primitives to maintain geometric fidelity at dense lattice intersections. No mid-print flow-rate adjustments were applied.

4.2 Application of the geometric framework

The wall geometry was defined using a staircase-based grading function applied over the 1.00 m wall length. Each layer was partitioned into three longitudinal density bands selected from $\{64, 32, 16\}$ subcell resolutions. The leftmost

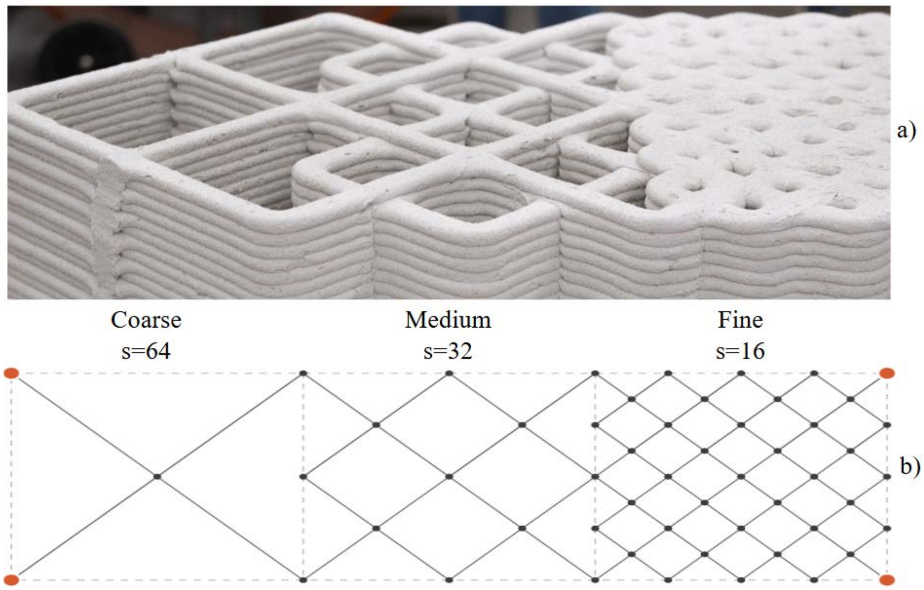

Fig. 2: (a) Detail of the top six layers of the printed wall showing the three density regions. (b) Simplified diamond-cell grading sketch illustrating how the lattice interconnects across density bands.

macrocell column remained fully dense across all layers, while upper layers progressively transitioned toward lighter lattice resolutions. For each layer k, the band field $B^{(k)}$ was expanded into diamond "X" subcells, producing a planar lattice graph with deterministic connectivity and exactly four degree-1 boundary nodes. This banded application is shown in Fig. 2.

4.3 Application of the Eulerian toolpath framework

Each layer graph was converted into a single continuous deposition path described in Section 3. Start–stop assignments alternated across layers, co-locating the next layer's start with the previous layer's end, which allowed the per-layer Eulerian paths to combine into a single global toolpath spanning all 35 layers.

5 Results

A functionally graded lattice wall measuring $1.00 \times 0.60 \times 0.35$ m was fabricated using a single uninterrupted Eulerian toolpath across 35 layers with no retractions. Deposition was executed at constant flow ($Q = 2.8$ L/min) with commanded speeds ranging from 0.1675–0.2094 m/s. The print duration was 2871 s (47 min 51 s), corresponding to an estimated toolpath length of ~ 520 m, extruded volume of 134 L (0.134 m^3), and deposited mass of ~ 295 kg. The wall reproduces the prescribed horizontal and vertical grading without toolpath discontinuities.

5.1 Implications for continuous concrete deposition

While mechanical testing was outside the scope of this study, prior work has demonstrated strong dependence of interlayer strength on deposition continuity [7]. The fabrication results demonstrate that enforcing Eulerian traversability enables continuous extrusion of a functionally graded lattice without start–stop events or flow interruptions. Maintaining a constant volumetric flow throughout the 35-layer build allowed the material to be deposited under consistent rheological conditions, which is critical in extrusion-based concrete printing where pauses and restarts are known to degrade interlayer bonding and introduce weak interfaces.

References

1. Jianzhuang Xiao, Guangchao Ji, Yamei Zhang, Guowei Ma, Viktor Mechtcherine, Jinlong Pan, Li Wang, Tao Ding, Zhenhua Duan, and Shupeng Du. Large-scale 3d printing concrete technology: Current status and future opportunities. *Cement and Concrete Composites*, 122:104115, 2021.
2. Dhrutiman Dey, Vuong Nguyen Van, H. Nguyen Xuan, Dodda Srinivas, Biranchi Panda, and Phuong Tran. Flexural performance of 3d printed concrete structure with lattice infills. *Developments in the Built Environment*, 16:100297, 2023.
3. Qian Wan, Wenwei Yang, Li Wang, and Guowei Ma. Global continuous path planning for 3d concrete printing multi-branched structure. *Additive Manufacturing*, 71:103581, 2023.
4. Man Chen, Xianhua Yao, Lu Zhu, Meishan Yin, Yan Xiong, and Nan Hu. Geometric design and performance of single and dual-printed lattice-reinforced cementitious composite. *Cement and Concrete Composites*, 143:105266, 2023.
5. Luca Breseghello, Hamidreza Hajikarimian, and Roberto Naboni. 3DLightSlab: Design-to-3d concrete printing workflow for stress-driven ribbed slabs. *Journal of Building Engineering*, 91:109573, 2024.
6. T. T. Le, S. A. Austin, S. Lim, R. A. Buswell, A. G. F. Gibb, and T. Thorpe. Mix design and fresh properties for high-performance printing concrete. *Materials and Structures*, 45(8):1221–1232, 2012.
7. R.J.M. Wolfs, F.P. Bos, and T.A.M. Salet. Hardened properties of 3d printed concrete: The influence of process parameters on interlayer adhesion. *Cement and Concrete Research*, 119:132–140, 2019.
8. Femke P. Bos, Rob J. M. Wolfs, Zeina Y. H. Ahmed, and Theo A. M. Salet. The realities of additively manufactured concrete structures: Projections and challenges. *Cement and Concrete Research*, 154:106718, 2022.
9. Luca Breseghello and Roberto Naboni. Toolpath-based design for 3d concrete printing of carbon-efficient architectural structures. *Additive Manufacturing*, 56:102872, 2022.
10. Prashant Gupta, Bala Krishnamoorthy, and Gregory Dreifus. Continuous toolpath planning in a graphical framework for sparse infill additive manufacturing. *Computer-Aided Design*, 127:102880, 2020.
11. Yamin Li, Kai Tang, Dong He, and Xiangyu Wang. Multi-axis support-free printing of freeform parts with lattice infill structures, 2020.